International Journal of Marine Engineering Innovation and Research, Vol. 11(2), Jun. 2026. 383-396
(pISSN: 2541-5972, eISSN: 2548-1479)

Anchorage Offset Sensitivity Analysis of a Single Point Mooring System with a Moored Crude Oil Tanker in the Gulf of Guinea

Oghenethoja M. Umuteme[1]*, Charles U. Orji[2] and Augustine A. Elakpa[3]

(Received: 10 March 2026 / Revised: 20 March 2026 / Accepted: 7 April 2026 / Available Online: 3 June 2026)

***Abstract*—** Deepwater Single Point Mooring (SPM) systems increasingly use Steel Catenary Risers (SCRs) for high-pressure hydrocarbon transfer in water depths greater than 500 m. However, the high axial stiffness of SCRs creates strong coupling between seabed anchors and the surface buoy, which can significantly affect system stability. This challenge is more critical in swell-dominated regions such as the Gulf of Guinea, where long-period waves induce large surge motions of moored tankers. This paper aims to achieve five objectives. First, to develop a coupled SPM–SCR–tanker numerical model. Second, to investigate the effect of anchorage offset on riser tension redistribution. Third, to quantify the contribution of risers to global restoring forces acting on the SPM. Fourth, to evaluate the influence of riser-induced loads on buoy hydrostatic stability. Fifth, to identify critical geometric thresholds governing stiffness transition. A six-degree-of-freedom time-domain model was developed in ANSYS Aqwa. The system consists of a cylindrical SPM buoy connected to a tanker by a polyester hawser and restrained by six SCRs. Simulations were carried out for anchor offsets ranging from 500 m to 2,000 m under representative swell conditions. The results show a nonlinear system response as the SCRs transition from catenary to semi-taut configurations. Riser tension increases significantly at large offsets, especially in aligned lines. The risers contribute substantially to horizontal restoring forces and generate downward loads on the buoy. These loads may exceed buoyancy capacity and reduce hydrostatic stability. Critical offset ranges of 1,000–1,500 m define the stiffness transition zone.

Keywords— Single Point Mooring (SPM), Very Large Crude Carriers (VLCCs), Steel Catenary Riser (SCR), Dynamic stability, Anchorage offset, Low-frequency swell response, time-domain, polyester hawser.

Corresponding Author: umonthoja@gmail.com

I. INTRODUCTION

The escalating global demand for hydrocarbons, coupled with the maturation of shallow-water basins, has positioned deepwater exploration and production as a cornerstone of the modern energy landscape [1]. Regions such as the Gulf of Guinea (GoG), the Brazilian Santos Basin, and the Gulf of Mexico have become key operational hubs, with developments extending beyond 500 m water depth into ultra-deepwater regimes. These environments impose stringent requirements on offshore infrastructure, particularly in ensuring the reliability and safety of fluid transfer systems under complex environmental loading.

Single Point Mooring (SPM) systems are widely employed for offshore loading operations, providing a flexible interface between subsea production systems and shuttle tankers [1], [2].

In deepwater applications, Steel Catenary Risers (SCRs) are commonly used to connect the seabed to the floating buoy due to their robustness and suitability for high-pressure flowlines [1], [3]. However, unlike compliant mooring systems, SCRs introduce high axial stiffness, resulting in strong coupling between the buoy, risers, and moored vessel [3], [4]. This coupling fundamentally alters the system's global response by enabling direct transmission of environmental and operational loads across the entire configuration.

Previous studies have extensively investigated the hydrodynamic response of SPM systems and the behaviour of moored vessels under environmental loading. For instance, tanker surge response in long-period swell conditions has been shown to dominate mooring loads, particularly in regions such as the Gulf of Guinea where peak wave periods range from 12 to 20 s [5], [6]. These studies highlight the importance of low-frequency vessel motions in driving extreme line tensions and hawser loads. Parallel research on SCR systems has focused on fatigue, vortex-induced vibration, and static configuration characteristics, emphasizing the transition between catenary and taut geometries as a key factor influencing tension response [3], [7].

Despite these advances, existing literature largely treats the SPM mooring system and SCR behaviour as separate or weakly coupled problems. Mooring analyses often assume quasi-static or compliant line behaviour, neglecting the stiffness-induced coupling effects introduced by SCRs. Conversely, SCR studies typically consider fixed or simplified boundary conditions at the floating interface, without accounting for coupled vessel–buoy dynamics. As a result, the integrated response of a coupled SPM–SCR–tanker system remains insufficiently understood, particularly under swell-dominated conditions.

A critical parameter that has received limited attention

Oghenethoja M. Umuteme with Centre of Excellence in Marine and Offshore Engineering, Rivers State University, Port Harcourt, Nigeria Email: umonthoja@gmail.com

Charles U. Orji with Centre of Excellence in Marine and Offshore Engineering, Rivers State University, Port Harcourt, Nigeria Email: orji.charles@ust.edu.ng

Augustine A. Elakpa with Department of Marine and Offshore Engineering, Rivers State University, Port Harcourt, Nigeria Email: augustine.elakpa@ust.edu.ng

in this coupled context is the anchorage offset distance. The anchor offset governs the initial riser geometry, hang-off angle, and effective stiffness of the SCR system [7], [8]. Variations in offset can significantly alter load distribution among risers, induce asymmetric tension patterns, and modify the global restoring characteristics of the mooring system. However, systematic sensitivity analyses linking anchorage offset to riser tension redistribution, restoring force generation, and buoy stability are scarce. In particular, the contribution of SCRs to global restoring forces—traditionally attributed primarily to mooring lines—remains poorly quantified.

Furthermore, the vertical load components induced by inclined SCRs introduce additional complexity by directly affecting the hydrostatic stability of the SPM buoy. While buoy stability is typically assessed using hydrostatic restoring parameters, the influence of riser-induced vertical forces is often neglected. This omission can lead to non-conservative designs, especially in cases where large tanker-induced loads amplify riser tensions and generate significant downward forces. The potential for stiffness transition—from seabed-supported catenary to semi-taut configurations—further introduces nonlinearities that may define critical operational limits, yet these geometric thresholds are not well established in current design practice.

In light of these gaps, this study performs an anchorage offset sensitivity analysis of a coupled SPM–SCR system with a moored crude oil tanker under Gulf of Guinea environmental conditions. The objectives are to:

1. Develop a coupled numerical model of a deepwater SPM–SCR–tanker system capable of capturing the interaction between the buoy, the polyester hawser connection, which is primarily used to connect the tanker to the bouy [9], and a six-point SCR mooring configuration.
2. Examine the effect of anchorage offset on riser tension redistribution, with particular emphasis on identifying how riser orientation relative to the displacement direction influences load concentration within the mooring spread.
3. Quantify the resulting global restoring forces acting on the SPM, including the horizontal forces generated by the riser system and their contribution to overall system stiffness.
4. Assess the influence of riser-induced loads on buoy hydrostatic stability, particularly the vertical loading effects that arise from increased riser tension under large offsets.
5. Identify critical geometric thresholds at which the SCR system transitions from a compliant seabed-supported catenary configuration to a stiffness-dominated regime associated with rapid tension amplification and reduced system stability.

Through these objectives, the study seeks to bridge the gap between traditional mooring load analysis and buoy stability assessment by providing a coupled evaluation framework for deepwater SCR-connected SPM systems.

The findings provides a quantifiable basis for optimizing mooring configurations to ensure the hydrodynamic stability and operational integrity of deepwater SPM systems subjected to the extreme, low-frequency loads characteristic of the Gulf of Guinea.

II. METHOD

The methodological framework for this numerical investigation is designed to systematically evaluate the influence of anchorage offset and hawser length on the dynamic stability of a deepwater Single Point Mooring (SPM) system. This section details the modelling approach, numerical setup, parametric variations, and analytical procedures employed to ensure the reproducibility and validation of the study.

2.1. Geometry and Modelling Approach

The numerical model comprises two primary components: the SPM buoy and the shuttle tanker. The SPM buoy is modelled as a cylindrical structure with a diameter of 20 m and a height of 5.4 m, with a conical extension of 8.6 m housing the crude oil pipeline flange connection. The shuttle tanker has a has an equivalent volumetric displacement of 1,787 m^3. All geometries (Figure 1) were developed and prepared within ANSYS DesignModeler, ensuring seamless integration and accurate representation for the subsequent hydrodynamic analysis. The dimensions of the SPM and Tanker are presented in Figures 2 and 3.

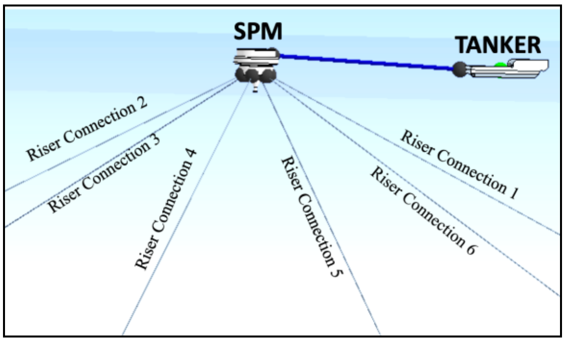

Figure 1. SPM and Crude Oil Tanker Mooring and Connection Arrangement

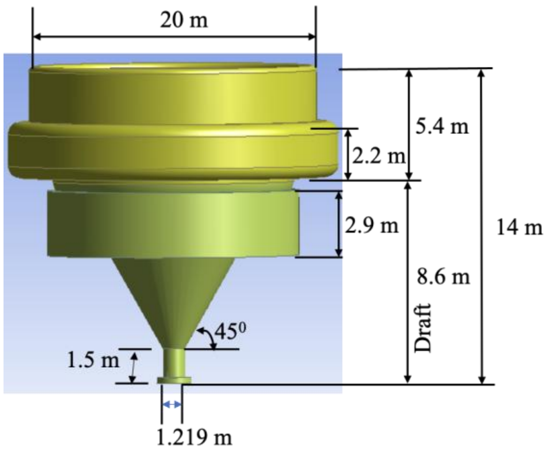

Figure 2. SPM Dimensions

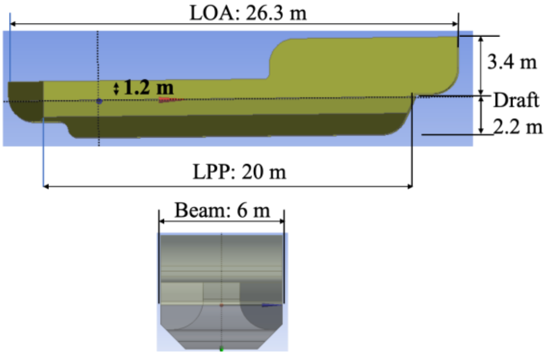

Figure 3. Tanker Dimensions

To maintain computational efficiency while accurately capturing the primary physical phenomenon—the inertial loading on the SPM—the tanker is modelled as a point mass with 6-degrees of freedom. This simplification focuses the analysis on the inertial effects of the tanker's low-frequency surge motions on the moored buoy, which is the core mechanism driving the overturning risk [6], [10].

For the SPM, the integrated turret system combined with spread mooring legs (Figure 1) allows the tanker to weathervane freely about the mooring system [9], rotating around the anchored legs in response to environmental loading (wind, waves, and current).

2.2. Meshing Strategy and Computational Domain

A structured mesh was generated for the SPM buoy's diffracting surface. A global mesh element sizing of 0.4 was adopted. This mesh density was selected as an optimal balance between numerical accuracy and computational expense, particularly respecting the limit for the hydrodynamic diffraction analysis in ANSYS Aqwa to ensure solution stability and efficiency. The computational domain, defined by its X/Y spread, was scaled to accommodate anchor offsets up to 2,000 meters at a uniform water depth of 500 meters. This provides a realistic operational envelope that captures the full range of the parametric study on the mooring footprint.

2.3. Mooring and Riser Configuration

The station-keeping system consists of six Steel Catenary Risers (SCRs) arranged in a symmetric 6-point spread mooring configuration. The risers are spaced at regular angular intervals of $\theta i = 60°$ around the SPM buoy, a robust and common design for deepwater applications. The material properties of the SCRs (Table 1) were defined to accurately reflect their high axial stiffness, a critical characteristic that governs the dynamic coupling between the buoy and the seabed [10]. Pre-tension in the risers was initialized based on their self-weight and the specified anchor offsets, establishing the static equilibrium position for the buoy prior to the application of environmental and tanker loads.

For all SCR configurations, the material and geometric properties were kept constant. The steel density was taken as 7,850 kg/m³ and Young's modulus as 210 GPa. The pipe had an outer diameter of 12 in and a wall thickness of 22 mm. The transverse drag coefficient was assumed to be 0.75, and the added mass coefficient was set to 1.0.

The directly pre-tensioned length of the riser was calculated using:

$$L_{scr} = \sqrt{\left({L_{offset}}^2 + {H_{seabed}}^2\right)} \quad (1)$$

For an offset distance of 1,000 m, this results in a pre-tensioned length of 1118 m and a touchdown angle α of 26.6^0. The SCR tension due to self-weight (Wscr) while neglecting hydrodynamic effect was estimated as:

$$T_0 = {W_{scr}}/{Sin\alpha} \quad (2)$$

The self-weigh is estimated using: $W_{scr} = \rho_{scr} V_{scr}$

Where ρ_{scr} ois the density of the SCR (7850 kg/m³) and V_{scr} is the volume of the steel calculated as:

$$V_{scr} = \frac{\pi({d_o}^2 - {d_i}^2)}{4} L_{scr} \quad (3)$$

Where d_o and d_i are the outside and inner diameters of the SCR respectively. The axial stiffness at the hang-off load-transferring interface, where the maximum stress occurs [8] at the SPM was calculated using:

$$K_{scr} = \frac{EA}{L_{scr}} \quad (4)$$

For the 12 inches SCR, and Young's Modulus of 210 GPa, EA = 3.84 GN, the K_{scr} at the fairlead is based on the suspended length of the SCR L_{scr}. In the Touch-Down Zone (TDZ), the "active" length of pipe being stretched is much shorter because the rest is supported by the soil. The study considered a 100 m active segment length of the SCR near the touchdown point, and was used in estimating the K_{scr}at the TDZ.

The axial stiffness is expressed as a spring constant. The mooring connection between the SPM and the Tanker is achieved through a Polyester rope of 120 mm diameter, with Young's Modulus of 4GPa, and a cross-sectional area of 0.0113 m^2.

$$K_{Hawser} = \frac{EA}{L_{Hawser}} \quad (5)$$

Where L_{Hawser} is varied from 45 m to 100 m. For a hawser length of 60 m, this gives a K_{Hawser} of 0.753GNm.

2.4. Point Mass

SPM Geometry and Mass Analysis: The design now features a 18 m wide "shoulder" at the waterline and a 45^0 narrow "keel." This geometry is highly effective for deepwater stability as it keeps the Waterplane Area large while reducing the Added Mass of the submerged lower section. The total surface area of the SPM is 1,271.7m^2. Therefore, the structural mass of steel based on the density of 7850kg/m^3 and a thickness of 30 mm, is 299, 485kg. The total point mass considering 20% for ancillary equipment is 359,382kg. Based on the conical section, the centre of gravity (CoG), KG is estimated to be located at the mid of the turret section, which is 6.0 m. The mass moment of inertia [11] was estimated using the parallel-axis theorem as follows:

$$I_{xx} = \sum(\bar{I}_{xx} + md^2) \quad (6)$$

Since the body is symmetrical on the XY plane, I_{xx} = I_{yy} = 13,183,000 kg.m^2. I_{zz} is approximated as mR^2. By taking an average radius of 8.5 m at the waterline, I_{zz} = 359,382 x 8.5 = 3,054,747 kg.m^2.

Crude Oil Tanker: The tanker is represented as a high-inertia Point Mass body to simulate its "hammer effect" on the mooring system during long-period swells. The mass moment of inertia was calculated using:

$$I = mK^2 \quad (7)$$

Where, c is the radius of gyration. For the vessel, K_{xx} is taken as 0.35Beam; K_{yy} and K_{zz} as 0.25LOA. The LOA of the Tanker is 26.3 m from Figure 3. The volume displacement ∇, is calculated as follows:

$$\nabla = C_B L_{pp} BT \quad (8)$$

Where $C_B$is the Block coefficient taken as 0.8; L_{pp} is the length between perpendiculars which is 20 m from Figure 3; B and T are the extreme breadth underwater (6 m) and the mean draft (2.2 m), respectively. This gives a volume displacement of 211.2 m^3. When filled with crude oil of 850kg/m^3 density, the total mass displacement will be (7850+850) x 211.2 =1,831,104 kg. Therefore, I_{xx}= 8,075,168.64kg.m^2. I_{yy}=I_{zz}= 79,159,770.36 kg.m^2.

2.5. Numerical Analysis Software: ANSYS Aqwa

All numerical simulations were performed using ANSYS Aqwa (Student edition), a suite of integrated modules specifically designed for the hydrodynamic analysis of offshore structures. The choice of Aqwa is justified by its proven capability in handling coupled dynamic responses of multiple floating bodies and complex mooring systems [12], backed by years of development and validation. The analysis settings for both diffraction and response were left at default. Hydrodynamic response is set to stability analysis. Simulation was achieved through 2.6 GHz 6-Core Intel Core i7 parallel processing, with RAM size of 32 GB 2667 MHz DDR4. All simulations were conducted using the Aqwa Theory Manual [13] as guide.

This study employs a parametric analysis to quantify how variations in anchorage offset influence load redistribution, riser tension development, and the resulting stability characteristics of the SPM–SCR system.

2.6. Environmental Conditions

The environmental loading was defined to represent the extreme long-period swell conditions characteristic of the Gulf of Guinea [14]. The wave climate was modelled using the JONSWAP-Glenn spectra with a peak enhancement factor (γ) of 3.3 [14]. This spectrum is widely accepted for describing fetch-limited, developing seas and is suitable for representing the long-period swells prevalent in the region. The significant wave height (Hs) ranges from 0.4 m to 2.5 m and spectral frequency ranges from 0.05 Hz to 0.25 Hz, with concentrations around 0.1 Hz [14]. Peak period (Tp) was selected to represent a design sea state with Tp of 20 s, with most significant period at 16 s. These long-period swells can excite resonant low-frequency surge motions in large tankers, leading to substantial hawser loads. The mean wave direction is predominantly 180^0, and wave height concentrated at 1.5 m, with peaks at 2 – 3 m. The spectrum co-linear wind and current were included as steady mean forces in the analysis [12]. The measured maximum wind speed is 10 m/s [14]. The wave velocities were calculated using the formulation for group velocity, c_g for ocean waves:

$$c_g = \frac{gT}{4\pi} \quad (9)$$

This gives a peak velocity of 15.6 m/s and a minimum wave velocity of 3.1 m/s. The sea state was at a sea forward speed of 2.0 m/s.

The simulation was executed for 500 iterations, by which point the numerical solution had reached convergence. This was confirmed by the stabilization of the monitored response variables and the flattening of the iteration history curves, indicating negligible changes between successive iterations.

2.7. Output Parameter Extraction and Evaluation Criteria

For each simulation case defined by a unique anchorage offset configuration, key system response parameters were extracted from the time-domain solutions generated in the hydrodynamic solver. The primary outputs included hawser tension at the tanker–SPM connection, axial tension in each of the six SCR legs, the resultant horizontal restoring force acting on the buoy, and the vertical displacement of the SPM relative to the still-water level. These parameters were selected because they directly characterize the load transfer mechanisms governing system stability. The extracted data were subsequently evaluated against two principal performance criteria:

(i) structural integrity of the riser system, assessed through the magnitude and redistribution of axial tensions, and
(ii) hydrostatic stability of the buoy, evaluated through the resulting vertical displacement relative to the available freeboard.

The combined interpretation of these metrics enabled identification of offset conditions that transition the system from a compliant catenary regime to a stiffness-dominated configuration associated with excessive structural loading and reduced operational stability.

2.8. Connections and Fixed-Point Determination

The connection coordinates for the six Steel Catenary Risers (SCRs) were defined explicitly at both the SPM buoy and the seabed anchorage points.

At the SPM buoy, the riser hang-off locations were positioned at a vertical elevation of z=−3 m relative to the mean waterline. Six equally spaced connection points were distributed circumferentially on a horizontal circle of radius R_{spm}=4 m, centred at the buoy axis. The angular positions were defined as: $\theta i=0^0,60^0,120^0,180^0,240^0,300^0$.

The corresponding Cartesian coordinates were computed as: $xi=R_{spm}\cos\theta i$, $yi=R_{spm}\sin\theta$. At the seabed (z=−500 m), the anchor points were arranged in a symmetric radial configuration directly aligned with the buoy hang-off angles. The anchorage radius R_{anchor} was varied parametrically from 500 m and 2,000 m to investigate the influence of mooring footprint geometry. The seabed coordinates were defined as: $xi=R_{anchor}\cos(\theta i)$, $yi=R_{anchor}\sin(\theta i)$.

This configuration ensured geometric symmetry of the 6-point SCR spread while allowing systematic variation of anchorage offset distance.

The tanker–SPM connection was modelled using a polyester. The hawser attachment point on the SPM buoy was located at z =+3 m above the mean waterline to represent the fairlead elevation. On the tanker, the connection was defined at the forward hull centreline, 2 m above the waterline, consistent with typical bow loading arrangements.

2.9. Verification and Limitations

To ensure the reliability of the numerical results, a mesh convergence study was implicitly considered by selecting a mesh size that respects the element count limits and geometric enhancement. While the chosen mesh density of approximately 335,317 elements is deemed adequate for capturing the primary rigid-body dynamics, a more rigorous convergence study with finer meshes is recommended for future work to quantify discretization error. A key limitation of this methodology is the modelling of SCRs as quasi-static catenaries within Aqwa's standard mooring line library. This approach, while computationally efficient, does not fully capture complex dynamic phenomena such as dynamic bending stresses at the hang-off point, compression, or hysteretic behaviour at the touchdown point. To address this, the current study focuses on axial tension as the primary failure mode for the riser. Future investigations could employ a hybrid coupled analysis (e.g., Aqwa and OrcaFlex) to capture these higher-order dynamic effects for a more detailed stress assessment

III. RESULT AND DISCUSSION

3.1. Hydrostatics

The SPM hydrostatics analysis (Table 1) confirms that the buoy satisfies intact static stability requirements with a positive metacentric height of 0.25 m and symmetric restoring characteristics. The displacement, waterplane properties, and hydrostatic stiffness matrix are internally consistent. The stability level is moderate and consistent with accepted offshore practice for compliant SPM systems. No hydrostatic non-conformities are identified at the analysed draft condition. The second moment of area I of the waterplane around the rotation axis is estimated from the results as follows:

$$I = \nabla . \mathrm{BM} \qquad (10)$$

With a BM 0f 2 m and actual displacement of 248 m^3, I = 496 m^4. This high value shows that the buoy can resist rapid acceleration from waves, providing a more stable platform for the mooring hawser and attached tanker.

TABLE 1.
SPM HYDROSTATIC ANALYSIS (VALIDATION)

Parameter	AQWA Simulation Result	Typical Acceptable Practice	Assessment
GM	0.25m	0.2-1.0 m typical for SPM	PASS
Positive GM	Yes	Mandatory for stability	PASS
GM symmetry	GMX GMY	SPM buoy must be stable while rotating around its vertical axis	PASS
Heave stiffness	793 kN/m	Consistent with $p.g.A_{wp}$; A_{wp}=79m^2; where g=9.81m/s^2 and r is 1,025kg/m^3	PASS
BM magnitude	2.0m	Physically reasonable for geometry	PASS

The stability level is moderate and consistent with accepted offshore practice for compliant SPM systems. No hydrostatic non-conformities are identified at the analysed draft condition. Hence, the SPM maintains its position against transient wind or wave changes, forcing the tanker to properly weathervane (rotate around the buoy) in a steady manner.

The natural roll period T_0, also shows consistency with the measured range of wave spectra periods for the Gulf of Guinea. Using a radius of gyration K of 0.35 times the diameter of the buoy (20 m) as the practice in some shipyards [15], the roll period is calculated as below:

$$T_0 = 2\pi \frac{\mathrm{K}}{\sqrt{gGM}} \qquad (11)$$

This calculated natural period of 28 s, is above the maximum measured period of 20 s for the Gulf of Guinea. Which is desirable as it shifts roll away from short wind-wave energy.

3.2. Effect of Anchorage Offset

The anchorage offset distance was varied from 500 m to 2000 m to evaluate its influence on the SCR mooring system tension and the resulting overturning force in the 60 m cable connection between the SPM and the tanker. The analysis was conducted under a wave condition corresponding to the speed of 2 m/s, worst case frequency of 0.05 Hz (Tp = 20 s) and a wave heading of 180°.

In addition to assessing mooring and connection loads, the study recorded the actual position responses of the SPM and the total reaction forces at both the SPM and tanker connection points, enabling a comprehensive evaluation of how anchor offset position affects system stiffness, load transfer, and overall position actual response behaviour. To enhance the comparative analysis, the axial stresses at the SPM and seabed anchor points were kept constant, so that the simulation will determine the final stresses as a result.

3.2.1. Effect on Hawser Connection (SPM →Tanker)

Table 2 presents the variation in hawser tension at the SPM–tanker connection point for increasing system offsets. The initial tension T_0 provided by the hydrodynamic solver is 0 MN, indicating that the polyester hawser was modelled without initial pretension. Consequently, the reported change in tension ΔT reflects the load response generated purely by the geometric displacement of the tanker relative to the SPM. The ΔT column is informative, because it shows how much additional load the riser experiences due to the applied offset relative to its initial unloaded state.

TABLE 2.
HAWSER CONNECTION (SPM →TANKER)

Offset (m)	Point (x, y, z) (m)	Initial Tension T_0 (MN)	Final Tension T_1 (MN)	ΔT (MN)
500	65, 0, 2	0.00	-0.11	-0.11
1,000	65, 0, 2	0.00	-0.15	-0.15
1,500	65, 0, 2	0.00	-0.26	-0.26
2,000	65, 0, 2	0.00	-0.22	-0.22

The results show that increasing offset produces negative tension values, ranging from –0.11 MN at 500 m to –0.26 MN at 1500 m. Since a polyester hawser cannot sustain axial compressive fatigue loads [16], these values indicate a reduction in line stretch relative to the reference configuration, corresponding to slackening of the hawser rather than compression. The magnitude of this relaxation increases with offset up to 1500 m, suggesting that the tanker displacement reduces the effective elongation of the hawser and diminishes the restoring load transmitted to the SPM.

At 2000 m offset, the tension magnitude decreases slightly to –0.22 MN, implying a partial geometric realignment of the system that limits further relaxation of the line. Overall, the results indicate that when the hawser is installed without pretension, increasing offset primarily leads to loss of effective tension (Figure 4), resulting in a relatively compliant connection between the tanker and the SPM.

From an operational perspective, this behaviour highlights the importance of maintaining adequate pretension in polyester hawsers [17], as slack conditions can increase the likelihood of dynamic snap loading when the line re-engages under environmental forcing. The results is in line with the outcome in the literature [18], suggesting that introducing a controlled pretension level may improve load stability and enhance the overall mooring performance of the SPM–tanker system.

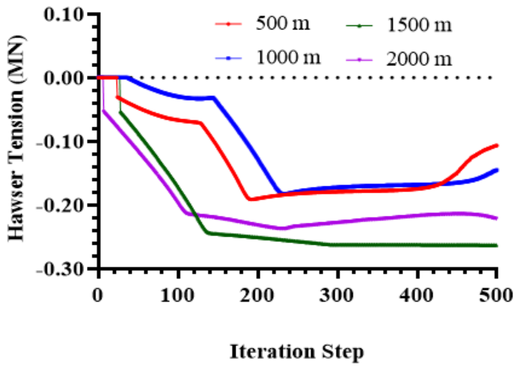

Figure 4. Hawser Connection Tension Plot

3.2.2. Effect on SCR Connections (SPM →Seabed Anchors)

Table 3 presents the variation in tension response of the first catenary riser leg as a function of seabed anchor offset in 500 m water depth. The results demonstrate a pronounced nonlinear increase in both final tension (T_1) and tension variation (ΔT) with increasing offset distance.

TABLE 3.
RISER CONNECTION 1 (SPM →SEABED ANCHOR 1)

Offset (m)	Point (x, y, z) (m)	Initial Tension T_0 (MN)	Final Tension T_1 (MN)	ΔT (MN)
500	500, 0, -500	-1.33	0.17	1.50
1000	1000, 0, -500	18.78	29.16	10.38
1500	1500, 0, -500	19.35	239.66	220.31
2000	2000, 0, -500	103.12	924.01	820.89

At 500 m offset, the riser exhibits near-slack behaviour, indicating significant seabed contact and low restoring stiffness. The negative initial tension suggests compression/slack dominance prior to load redistribution. In this regime, the mooring system behaves as a classical catenary with high compliance and limited load transfer to the anchor and hang-off point.

At 1,000 m offset, tension increases moderately, reflecting partial seabed lift-off and improved restoring capacity. The system remains catenary-dominated, with gradual load transfer from seabed support to axial tension. A critical transition occurs between 1,000 m and 1,500 m offset, where tension rises sharply (ΔT increases from 10.38 MN to 220.31 MN). This indicates progressive loss of seabed contact and a shift toward semi-taut behaviour. The riser stiffness increases geometrically as curvature reduces and horizontal tension becomes dominant.

At 2000 m offset, the riser approaches taut-line response, resulting in extreme tension amplification (T_1 = 924.01 MN) as seen in Figure 5. In this regime, the full suspended weight of the riser and increased horizontal restoring force are transferred to the hang-off point and anchor, significantly increasing structural demand.

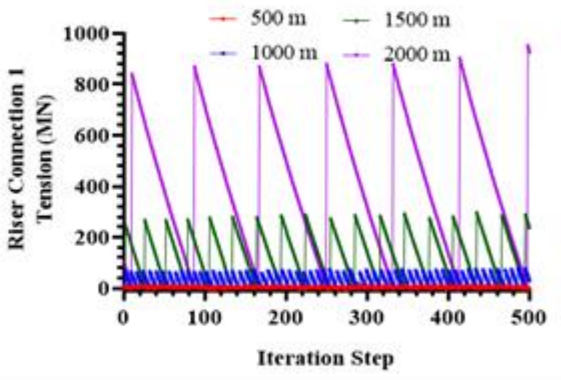

Figure 5. Riser Connection 1 Tension Plot

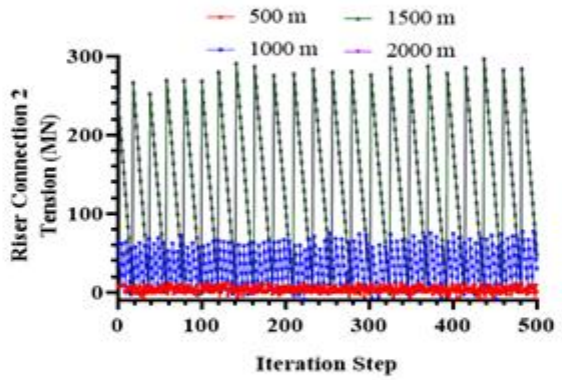

Figure 6. Riser Connection 2 Tension Plot

Operationally, these results highlight that excessive seabed anchor offset substantially increases hang-off tension and anchor loading, potentially compromising structural integrity and fatigue performance. An optimal offset therefore lies within the catenary-dominated region, where sufficient restoring stiffness is achieved without inducing excessive axial tension. Also, Table 4 presents the tension response of Riser Connection 2 under increasing seabed anchor offset in 500 m water depth. Unlike Riser Connection 1, this leg exhibits a consistent reduction in final tension relative to its initial tension across all offset distances, as indicated by the negative ΔT values. At 500 m offset, the riser experiences a moderate initial tension (8.15 MN), which decreases to 0.39 MN after system response (ΔT = −7.76 MN). This suggests load redistribution within the mooring spread on the turret system, where this connection sheds load during equilibrium adjustment.

TABLE 4.
RISER CONNECTION 2 (SPM →SEABED ANCHOR 2)

Offset (m)	Point (x, y, z) (m)	Initial Tension T_0 (MN)	Final Tension T_1 (MN)	ΔT (MN)
500	250, 433, -500	8.15	0.39	-7.76
1,000	500, 866, -500	62.74	30.13	-32.61
1,500	750, 1299, -500	249.8	48.00	-201.81
2,000	1;000,1732, -500	1,124	1,048	-75.63

As offset increases to 1,000 m and 1,500 m, the reduction in tension becomes more pronounced (ΔT = −32.61 MN and −201.81 MN, respectively). This behaviour indicates progressive load transfer from Riser Connection 2 to other mooring legs—particularly the leg aligned with the direction of offset. The system response reflects directional stiffness dominance, where the up-wave or aligned leg attracts higher tensile loads while opposing or inclined legs unload [19]. At 2,000 m offset, although the final tension remains high (1,048.37 MN), as seen in Figure 6, the reduction relative to initial tension is smaller in Table 4 (ΔT = −75.63 MN) compared to the 1500 m case. This suggests that the system has transitioned into a highly stiff, taut configuration, where all mooring legs begin to share elevated baseline tension due to geometric straightening and full lift-off from the seabed.

Table 5 shows that Riser Leg 3, located in the negative x-direction and positive y-direction relative to the SPM, is spatially inclined opposite to the primary offset direction. This orientation significantly influences its tension response as offset distance increases.

At 500 m offset, the leg experiences a slight increase in tension (ΔT = +9.06 MN), indicating minor load participation within a predominantly catenary and compliant configuration. However, at 1,000 m offset, tension drops substantially (ΔT = −63.18 MN), with the final tension approaching slack conditions. This reflects directional load redistribution toward the offset-aligned leg, reducing axial demand in Leg 3 due to its opposing horizontal orientation.

TABLE 5.
RISER CONNECTION 3 (SPM →SEABED ANCHOR 3)

Offset (m)	Point (x, y, z) (m)	Initial Tension T_0 (MN)	Final Tension T_1 (MN)	ΔT (MN)
500	-250, 433, -500	0.27	9.33	9.06
1,000	-500, 866, -500	62.74	-0.44	-63.18
1,500	-750, 1299, -500	249.81	141.29	-108.5
2,000	-1,000, 1732, -500	1,124	1,005	-119.3

As offset increases to 1500 m and 2000 m, the leg continues to exhibit net unloading (ΔT = −108.52 MN and −119.33 MN, respectively), despite high absolute tension levels at 2000 m as seen in Figure 7.

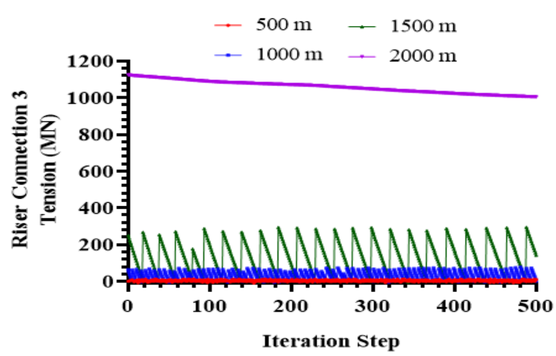

Figure 7. Riser Connection 3 Tension Plot

This behaviour indicates that while global system stiffening elevates overall tension in all lines under near-taut conditions, the dominant share of horizontal restoring force remains concentrated in the offset-aligned riser.

Overall, the results confirm that spatial orientation strongly governs load sharing in the mooring spread, with Leg 3 (X-axis, -30º) contributing progressively less to restoring capacity as directional stiffness effects intensify [20].

Table 6 illustrates the dynamic tension response of Riser Leg 4, which is oriented along the negative X-axis (180°) and connects the Single Point Mooring (SPM) buoy to Seabed Anchor 4 at a constant depth of z = −500 m. The coordinate points shown represent the displaced position of the SPM relative to the anchor as horizontal offset increases. At the 500 m offset, corresponding to the position (−500, 0, −500), the system exhibits an initial tension of T_0 = −1.33 MN, indicating compressive loading in the riser. Such negative tension suggests a high likelihood of compressive buckling, implying that the riser is insufficiently tensioned and the configuration is structurally unstable. As the offset increases to 1,000 m at (−1000, 0, −500), the riser begins to experience meaningful axial loading, with tension increasing from 18.78 MN to 45.33 MN, giving ΔT = 26.55 MN. This positive change reflects the gradual reduction of the catenary curvature as the horizontal distance between the SPM and the seabed anchor increases. A much stronger response occurs at 1500 moffset, represented by (−1500, 0, −500), where the final tension rises sharply to 272.50 MN, resulting in ΔT = 253.16 MN. This range between 1,000 m and 1,500 m clearly marks the transition from a slack-catenary regime to a taut stiffness-dominated regime, where the riser loses geometric flexibility and tension increases rapidly with additional displacement.

TABLE 6.
RISER CONNECTION 4 (SPM →SEABED ANCHOR 4)

Offset (m)	Point (x, y, z) (m)	Initial Tension T_0 (MN)	Final Tension T_1 (MN)	ΔT (MN)
500	-500, 0, -500	-1.33	-1.67	-3.00
1,000	-1,000, 0, -500	18.78	45.33	26.55
1,500	-1,500, 0, -500	19.34	272.50	253.16
2,000	-2,000, 0, -500	1,124.00	982.68	-141.32

At the extreme 2,000 m offset, corresponding to (−2,000, 0, −500), the system becomes significantly over-constrained, with the initial tension reaching 1,124.00 MN as seen in Figure 8, which is also similar to the concern in Figure 7. Although the final tension reduces slightly to 982.68 MN (ΔT = −141.32 MN), the magnitudes remain extremely high and indicate severe overstressing of the riser system.

From an operational perspective, these results highlight critical safety implications for tanker–SPM operations in environments such as the Gulf of Guinea, where long-period swells can induce large vessel excursions. The results suggest that offsets exceeding approximately 1,500 m may expose the riser to snap-loading, structural yielding, or catastrophic failure, while very small offsets may introduce instability through compressive buckling. Consequently, maintaining vessel excursions within a controlled operational envelope and ensuring adequate mooring stiffness are essential to prevent excessive tension development and to safeguard the structural integrity of the riser system [21].

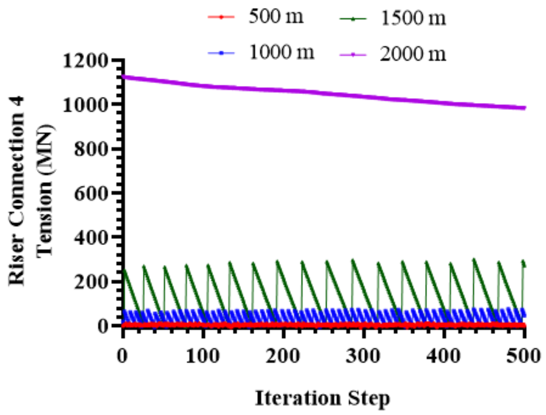

Figure 8. Riser Connection 4 Tension Plot

Table 7 presents the tension response of Riser Leg 5, which connects the Single Point Mooring (SPM) buoy to Seabed Anchor 5 and is oriented diagonally in the south-west direction of the horizontal plane, as indicated by the coordinate progression (x, y) = (−250, −433), (−500, −866), (−750, −1,299), and (−1,000, −1,732). These coordinates show that the displacement of the SPM occurs simultaneously along both the negative X and negative Y directions, while the anchor depth remains fixed at z = −500 m. This geometric orientation means that Riser Leg 5 experiences two-dimensional horizontal stretching, unlike riser legs aligned strictly along a single axis, and this has important implications for the observed loading behaviour.

TABLE 7.
RISER CONNECTION 5 (SPM →SEABED ANCHOR 5)

Offset (m)	Point (x, y, z) (m)	Initial Tensio n T_0 (MN)	Final Tension T_1 (MN)	ΔT (MN)
500	-250, -433, -500	0.27	1.39	1.12
1,000	-500, -866, -500	62.74	29.26	-33.48
1,500	-750, -1,299, -500	249.8	160.79	-89.02
2,000	-1,000, -1,732, -500	1,124	1,005	-119.3

At the 500 m offset, corresponding to the coordinate (−250, −433, −500), the riser experiences very small initial and final tensions (T_0 = 0.27 MN and T_1 = 1.39 MN) with ΔT = 1.12 MN, indicating that the line remains in a relatively relaxed catenary state. The small positive increase in tension suggests only minor geometric stretching as the buoy begins to move away from the anchor. However, as the offset increases to 1,000 m at (−500, −866, −500), the initial tension rises significantly to 62.74 MN, while the final tension drops to 29.26 MN, producing a negative ΔT of −33.48 MN. This reduction suggests that the riser undergoes load redistribution or geometric reconfiguration during the dynamic simulation, possibly as other mooring or riser elements begin to share the load.

A more pronounced effect is observed at 1500 m offset, represented by (−750, −1,299, −500), where the initial tension increases sharply to 2,49.81 MN, but the final tension reduces to 160.79 MN, resulting in ΔT =

−89.02 MN. The large magnitude of ΔT indicates significant dynamic adjustment within the system as the riser approaches a taut configuration, where stiffness rather than catenary geometry begins to dominate the structural response. At the extreme 2000 m offset, corresponding to (−1,000, −1,732, −500), the initial tension rises dramatically to 1,124.00 MN (see Figure 9), while the final tension decreases slightly to 1,004.67 MN, giving ΔT = −1,19.33 MN. These values suggest that the system becomes highly constrained, with tension levels approaching or exceeding the Minimum Breaking Load (MBL) of typical steel riser systems, indicating severe structural loading conditions.

The coordinate orientation provides additional insight into the comparatively high tension values observed. Because Riser Leg 5 is not aligned purely along the surge direction but instead lies along a diagonal azimuth, the buoy offset produces combined surge and sway components of displacement relative to the anchor. This increases the effective horizontal distance between the SPM and the anchor more rapidly than for a single-axis displacement, resulting in greater geometric stretching of the riser.

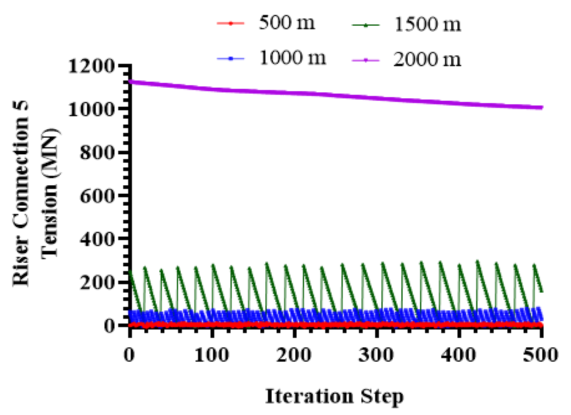

Figure 9. Riser Connection 5 Tension Plot

Consequently, the line experiences higher axial loads and earlier transition toward a taut configuration. From an operational standpoint, this behaviour is particularly important for tanker–SPM operations in the Gulf of Guinea, where multidirectional swell and current conditions can induce coupled surge–sway motions. Under such conditions, diagonal riser orientations such as Riser Leg 5 may experience higher effective loading and greater susceptibility to snap-loading or structural yielding when offsets approach or exceed 1,500 m.

This highlights the need to carefully consider riser orientation within the mooring layout and to maintain vessel excursions within safe operational limits to prevent excessive tension development [21].

Table 8 presents the simulated tension behaviour of Riser Leg 6, which connects the Single Point Mooring (SPM) buoy to Seabed Anchor 6 and is oriented along a south-east diagonal direction in the horizontal plane, as indicated by the coordinate sequence (250, −433), (500, −866), (750, −1,299) and (1,000, −1,732).

TABLE 8.
RISER CONNECTION 6 (SPM →SEABED ANCHOR 6)

Offset (m)	Point (x, y, z) (m)	Initial Tension T_0 (MN)	Final Tension T_1 (MN)	ΔT (MN)
500	250, -433, -500	0.27	-7.22	-7.49
1000	500, -866, -500	62.74	1.82	-60.92
1500	750, -1299, -500	249.81	70.67	-179.14
2000	1000, -1732, -500	1124.00	1048.37	-75.63

These coordinates show that as the vessel–SPM system offsets, the buoy moves simultaneously in the positive X-direction and negative Y-direction, while the anchor remains fixed at z = −500 m. This combined horizontal displacement influences the loading behaviour of the riser through geometric stretching and dynamic load redistribution within the mooring–riser system. At the 500 m offset, corresponding to the coordinate (250, −433, −500), the riser experiences a small initial tension (T_0 = 0.27 MN) but the final tension becomes −7.22 MN, producing ΔT = −7.49 MN. The negative final tension suggests that the riser transitions into a compressive or slack condition, indicating a strong possibility of local buckling or loss of effective tension in the line. This behaviour suggests that the riser is initially relaxed and that the imposed displacement does not sufficiently stretch the line to maintain stable tensile loading.

At an offset of 1,000 m, corresponding to (500, −866, −500), the initial tension increases significantly to 62.74 MN, but the final tension reduces sharply to 1.82 MN, resulting in ΔT = −60.92 MN. This large reduction in tension indicates that during dynamic adjustment the riser undergoes substantial load redistribution, likely transferring part of the load to neighbouring mooring components while the riser geometry reconfigures into a lower-energy catenary state.

A similar trend is observed at 1,500 m offset, represented by (750, −1,299, −500), where the initial tension rises to 249.81 MN, yet the final tension decreases markedly to 70.67 MN, producing ΔT = −179.14 MN. Although the line begins to approach a taut configuration, the large negative ΔT indicates that dynamic equilibrium within the system reduces the effective axial load carried by this particular riser leg. This suggests that the diagonal orientation of the line allows part of the surge-induced loading to be redistributed among other riser legs or mooring components.

At the extreme 2,000 m offset (see Figure 10), corresponding to (1,000, −1,732, −500), the riser reaches extremely high initial tension levels (T_0 = 1,124.00 MN) before relaxing slightly to a final tension of 1,048.37 MN, giving ΔT = −75.63 MN.

Although the final tension remains marginally lower than the initial value, the magnitude of these loads indicates that the riser system has entered a highly constrained regime, where geometric extension and structural stiffness dominate the response. Such loads approach or can exceed the Minimum Breaking Load (MBL) for typical steel riser systems and therefore represent a potentially critical operating condition.

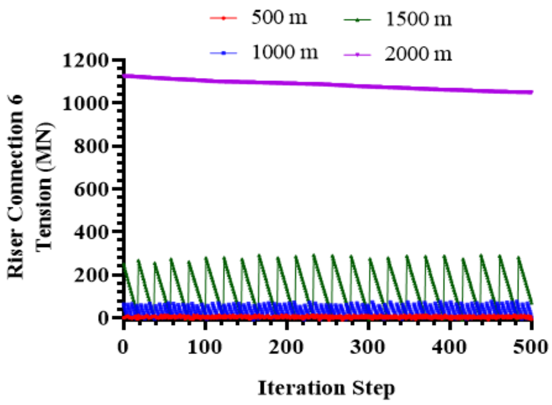

Figure 10. Riser Connection 6 Tension Plot

The coordinate orientation of Riser Leg 6 provides important insight into the observed behaviour. Because the line lies along a combined surge–sway direction (positive X and negative Y), the horizontal offset generates complex loading interactions with adjacent riser legs. In contrast to Riser Leg 5, which experienced increasing tension with offset, Riser Leg 6 demonstrates consistent negative ΔT values, dropping at 2,000 m offset, indicating that it tends to shed load during dynamic response rather than accumulate it. This suggests that the riser primarily acts as a secondary load-sharing element within the mooring configuration, with neighbouring lines likely carrying a larger portion of the surge-induced loads.

From an operational perspective, the results again highlight the sensitivity of the SPM–riser system to large vessel excursions in environments such as the Gulf of Guinea, where long-period swell and multidirectional wave action can produce coupled surge and sway motions. While moderate offsets may lead to temporary slack or load redistribution in some riser legs, extreme offsets approaching 2,000 m generate very high initial tensions that could result in snap-loading, structural yielding, or fatigue damage. Consequently, maintaining vessel position within safe offset limits and ensuring balanced load distribution among riser connections remain critical for preserving the structural integrity of the SPM mooring system.

3.2.3. Effect on Total Force Acting on SPM (Global X -Direction)

Table 9 summarizes the variation in the total horizontal force acting on the Single Point Mooring (SPM) in the global X-direction as the vessel–SPM system undergoes increasing offsets.

TABLE 9.
TOTAL FORCE ACTING ON SPM (GLOBAL X -DIRECTION)

Offset (m)	**Initial Force, F_0 (MN)**	**Final Force, F_1 (MN)**	**ΔF (MN)**
500	1.71	-7.04	-8.75
1,000	0.00	-12.00	-12.00
1,500	0.00	-94.63	-94.63
2,000	-1,006.32	-115.84	890.48

The results illustrate how the combined response of the mooring system and riser connections influences the net restoring force acting on the buoy as it is displaced from equilibrium. At an offset of 500 m, the system initially experiences a small positive force (F_0 = 1.71 MN), indicating a slight restoring tendency in the positive X-direction. However, after the dynamic response is accounted for, the final force becomes −7.04 MN, producing a change of ΔF = −8.75 MN. This reversal in force direction suggests that the combined action of the risers and mooring lines begins to pull the SPM back toward the equilibrium position along the negative X-direction.

As the offset increases to 1,000 m, the initial force becomes approximately zero, indicating that the system is near a neutral equilibrium state at the beginning of the simulation. The final force, however, reaches −12.00 MN, giving ΔF = −12.00 MN, which reflects the development of a stronger restoring force opposing the imposed displacement. This behaviour becomes significantly more pronounced at 1,500 m offset, where the final force increases in magnitude to −94.63 MN. The large negative value indicates that the mooring–riser system has entered a stiff response regime, where the combined stiffness of the lines generates a substantial restoring force resisting further displacement of the SPM.

At the extreme 2000 m offset, the system exhibits a very large initial force of −1,006.32 MN (see Figure 11), indicating that the mooring and riser network is already highly tensioned and strongly resisting further displacement.

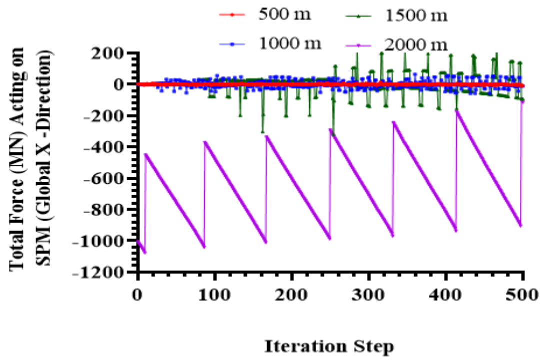

Figure 11. Total Force Acting on SPM (Global X -Direction)

During the dynamic response, the final force reduces significantly to −115.84 MN, producing a very large positive change of ΔF = 890.48 MN. This dramatic reduction suggests that the system undergoes substantial load redistribution and geometric adjustment as the structure approaches its mechanical limits. Such behaviour is consistent with the previously observed tension responses in individual riser legs, where extreme offsets lead to highly constrained configurations followed by partial relaxation as the system seeks a new equilibrium state.

From an operational perspective, these results demonstrate that increasing vessel offsets significantly amplifies the
restoring forces acting on the SPM, particularly beyond 1,000–1,500 m, where the mooring system

transitions from a relatively flexible catenary-dominated response to a stiff, tension-dominated regime. In operational environments such as the Gulf of Guinea, where long-period swell and environmental loading can induce large vessel excursions, excessive offsets may generate large horizontal forces that place substantial stress on the buoy structure, mooring lines, and riser connections. Maintaining vessel position within safe offset limits is therefore essential to prevent excessive global loading on the SPM system and to ensure the structural integrity and operational reliability of the offshore loading facility.

3.2.4. Effect on Actual SPM Position (Global Z -Direction)

Table 11 presents the response of the actual vertical position of the Single Point Mooring (SPM) buoy in the global Z-direction as the system experiences increasing horizontal offsets between the buoy and the SCR seabed anchors. In the coordinate system used in the simulation, the still water surface is defined at Z = 0 m, while the SPM has a freeboard of 5.4 m above the sea surface under equilibrium conditions. Consequently, downward displacement of the buoy reduces this available freeboard before any structural submergence occurs.

At an offset of 500 m, the final buoy position reaches −3.47 m, corresponding to a vertical displacement of $\Delta S = -3.47$ m. Although the buoy is pulled downward relative to the sea water surface, this displacement remains within the available freeboard allowance, meaning that the SPM deck would still remain approximately 1.93 m above the water level. This indicates that the mooring–riser system is still operating within a relatively flexible catenary regime, where the horizontal offset induces only moderate vertical loading.

TABLE 10.
ACTUAL SPM POSITION (GLOBAL Z -DIRECTION)

Offset (m)	Initial Position (m)	Final Position (m)	ΔS (m)
500	0.00	-3.47	-3.47
1000	0.00	-37.14	-37.14
1500	0.00	-80.57	-80.57
2,000	0.00	-206.68	-206.68

However, as the offset increases to 1,000 m, the final position drops significantly to −37.14 m, far exceeding the available freeboard. This result indicates that the vertical component of tension in the risers and mooring lines becomes sufficiently large to overcome the buoyancy restoring capacity of the SPM, effectively pulling the buoy deep below the sea surface. The effect becomes progressively more severe at 1,500 m and 2,000 m offsets, where the final vertical positions reach −80.57 m and −206.68 m, respectively. These large downward displacements (see Figure 12) indicate that the system transitions from a flexible catenary-controlled response to a highly constrained taut-line configuration, where increasing horizontal separation between the SPM and the SCR anchors generates large vertical force components.

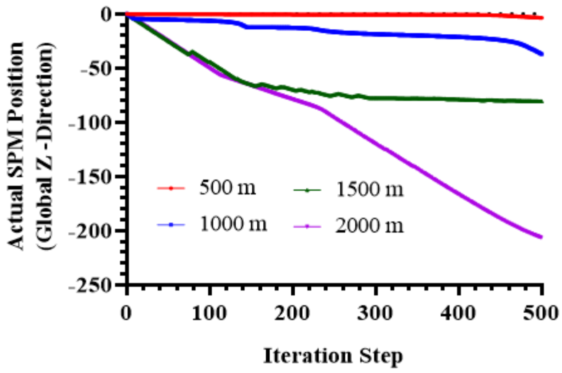

Figure 12. Actual SPM Position (Global Z -Direction)

From an operational perspective, these results clearly indicate that while small offsets such as 500 m can be accommodated within the buoy's freeboard allowance, larger offsets produce vertical forces that far exceed the buoyancy capacity required to maintain the SPM at the sea surface. Such conditions would be physically unacceptable in real operations, as the buoy must remain afloat to support tanker mooring and hydrocarbon transfer operations. The results therefore highlight the importance of maintaining vessel excursions within safe operational limits and ensuring that the geometric configuration of the SCR anchors does not induce excessive vertical loading on the SPM.

A critical offset threshold of 500 m was observed above which the SPM is submerged in the sea under the weight of the mooring risers.

3.3 Research Implications

The results presented in this study reveal a strong coupling between geometric offset and the mechanical behaviour of the integrated SPM–SCR system. The simulations demonstrate that the system response is highly nonlinear and governed primarily by the transition of the SCR configuration from a seabed-supported catenary regime to a semi-taut or taut-line regime as horizontal offset increases.

At smaller offsets (≤ 500 m), the risers retain significant seabed contact, allowing the system to redistribute loads through geometric compliance. In this regime, restoring forces remain relatively small and the buoy maintains vertical stability within the available freeboard. However, as offsets approach 1,000–1,500 m, the progressive lift-off of the SCRs from the seabed substantially increases axial tension, resulting in rapid amplification of both horizontal and vertical load components.

This transition highlights the importance of geometric configuration and anchor footprint in controlling system stiffness. Once the risers approach a taut configuration, the ability of the system to dissipate displacement through catenary curvature is lost, and loads are transferred directly through axial tension. The resulting stiffness escalation produces large restoring forces and strong vertical coupling, which can exceed the buoyancy capacity of the SPM.

From a research perspective, these findings emphasize the need for integrated mooring–riser analysis frameworks when evaluating deepwater loading systems. Treating the risers and mooring elements independently can lead to underestimation of the nonlinear load amplification associated with large geometric offsets.

3.4 Design Implications

The numerical results provide several important insights for the design of SPM systems operating with steel catenary risers in deep water.

First, the analysis demonstrates that riser orientation relative to the offset direction strongly governs load sharing within the mooring spread. Risers aligned with the displacement direction experience significant tension amplification, while opposing risers progressively unload. This directional load concentration suggests that symmetric riser layouts may still produce highly asymmetric load distributions during large excursions. Designers must therefore ensure that the maximum allowable tension in the most critically aligned riser governs the system design.

Second, the observed escalation in horizontal restoring forces with increasing offset indicates that the effective stiffness of the system is controlled primarily by the riser geometry rather than the hawser connection. As the risers transition toward taut configurations, restoring forces increase rapidly, imposing large structural loads on the buoy, turret, and riser hang-off structures. The results therefore highlight the importance of careful optimization of anchor radius and riser length to maintain sufficient geometric compliance within the operating envelope.

Third, the vertical displacement results demonstrate that excessive horizontal offset can generate large downward force components through riser tension, potentially exceeding the buoyancy capacity of the SPM. The simulations indicate that offsets exceeding approximately 1000 m may produce vertical loads capable of submerging the buoy below the free surface, which would be unacceptable for practical offshore loading operations. This finding suggests that the allowable geometric offset should be constrained to maintain a safe margin between riser-induced vertical forces and available buoyancy restoring capacity.

Finally, the hawser results indicate that the polyester connection behaves as a highly compliant element when installed without pretension. Although this compliance may reduce peak loads transmitted to the tanker, it also allows the line to slacken under displacement. Introducing a controlled pretension level would improve load transfer stability and reduce the risk of snap loading [17].

3.5 Operational Implications

The system behaviour observed in the simulations also carries several important operational implications for offshore loading operations.

The slackening of the polyester hawser at increasing offsets indicates that tanker–SPM load transfer becomes progressively less stable as the separation distance grows. In operational conditions where wave and swell motions are present, a slack hawser can experience cyclic re-tensioning, which may generate high dynamic snap loads that exceed the static tensions observed in the present simulations. Maintaining adequate pretension or limiting tanker excursion distance may therefore be necessary to ensure safe loading operations [17].

The strong directional load concentration observed in the SCR spread also implies that environmental conditions producing sustained drift in a particular direction—such as persistent wind or current—could significantly increase tension in one or two critical risers. Continuous monitoring of riser tension and buoy motion may therefore be required to prevent localized overstressing during prolonged loading operations.

Finally, the large downward displacements predicted for offsets beyond 1,000 m highlight the operational risks associated with excessive vessel drift during cargo transfer. Significant buoy submergence could compromise deck equipment, loading arms, and hose connections, potentially leading to hazardous operating conditions. Establishing operational excursion limits for the tanker relative to the SPM is therefore essential to ensure that the mooring–riser system remains within a safe mechanical regime.

IV. CONCLUSION

This study developed and applied a coupled numerical analysis to investigate the structural and stability behaviour of a deepwater Single Point Mooring (SPM) system connected to a tanker and a six-leg Steel Catenary Riser (SCR) mooring configuration. The conclusions drawn from the numerical simulations are presented in alignment with the study objectives.

4.1 Development of a coupled SPM–SCR–tanker numerical model

A coupled numerical model was successfully developed to represent the integrated behaviour of the SPM, polyester hawser, and six-point SCR mooring configuration. The model effectively captured the interaction between tanker displacement, hawser load response, riser tension redistribution, and the resulting global forces acting on the buoy. Simulation outputs demonstrated that the modelling framework can reproduce the nonlinear mechanical behaviour of the mooring–riser system under large geometric offsets, providing a robust analytical platform for evaluating deepwater SPM stability and load transfer mechanisms.

4.2 Effect of anchorage offset on riser tension redistribution

The results clearly demonstrate that anchorage offset strongly governs the redistribution of tension within the SCR mooring spread. Riser legs aligned with the direction of displacement experienced pronounced tension amplification as offset increased, transitioning from a slack seabed-supported catenary configuration to a semi-taut and eventually near-taut configuration. Conversely, riser legs oriented opposite or oblique to the displacement direction progressively shed load, exhibiting negative changes in tension. This directional load concentration confirms that riser orientation relative to the displacement vector is a dominant factor controlling the structural demand within the mooring system.

4.3 Contribution of risers to global restoring forces acting on the SPM

The study quantified the global horizontal restoring forces acting on the SPM and showed that these forces increase nonlinearly with increasing anchor offset. At small offsets, the riser system behaves as a compliant catenary structure with limited horizontal stiffness. However, as offsets increase and the risers progressively lift off the seabed, the system stiffness increases significantly, resulting in a sharp rise in horizontal restoring forces. These forces become particularly large beyond approximately 1500 m offset, indicating that the SCR system becomes the dominant contributor to overall system stiffness and structural loading on the buoy and turret assembly.

4.4 Influence of riser-induced loads on buoy hydrostatic stability

The simulations reveal that the vertical components of riser tension have a substantial influence on the hydrostatic stability of the SPM. At moderate offsets, the buoy remains within its available freeboard limits, indicating that buoyancy restoring forces are sufficient to counteract the vertical components of riser tension. However, as the risers transition toward taut configurations, the vertical tension components increase dramatically, producing large downward forces that exceed the buoy's buoyancy capacity. The predicted downward displacements of the buoy at offsets beyond 1,000 m demonstrate that riser-induced loads can significantly compromise buoy hydrostatic stability if system geometry is not properly controlled.

4.5 Identification of critical geometric thresholds for stiffness transition

The numerical results identify a critical geometric threshold between approximately 1,000 m and 1500 m of anchor offset at which the SCR system transitions from a compliant catenary-dominated regime to a stiffness-dominated configuration. Within this range, rapid amplification of riser tension occurs, accompanied by a sharp increase in global horizontal restoring forces and significant vertical loading on the SPM. Beyond this threshold, the mooring–riser system becomes structurally over-constrained, with the offset-aligned riser carrying a disproportionate share of the load and the buoy experiencing extreme downward forces. This transition represents a critical limit for safe operational geometry in deepwater SPM systems.

Overall, the study demonstrates that the mechanical behaviour and stability of SCR-connected SPM systems are strongly controlled by the geometric relationship between the buoy and the riser anchor locations. Increasing offsets produce a coupled escalation in riser tension, global restoring forces, and vertical loading on the buoy. Once the system approaches the stiffness dominated regime, the risk of excessive structural loading and loss of buoy stability increases significantly. The coupled modelling framework developed in this study therefore provides a quantitative basis for optimizing mooring configurations and anchor placement to maintain hydrodynamic stability and operational integrity of deepwater SPM systems operating under the low-frequency environmental loads characteristic of the Gulf of Guinea.

Further research should focus on the following two complementary areas to enhance the understanding and operational safety of deepwater SPM–SCR systems:

1. Extend the current quasi-static simulations to include fully coupled time-domain analyses under realistic environmental conditions, including waves, wind, and currents, to capture transient effects on riser tension redistribution and buoy motion.
2. Investigate the influence of controlled pretension in the polyester hawser on mitigating slack-induced dynamic snap loads, particularly under large offset excursions, to improve tanker–SPM load transfer reliability.

ACKNOWLEDGEMENTS

The authors acknowledge Rivers State University's Centre of Excellence in Marine and Offshore Engineering for providing computational resources and technical support. The author also acknowledges SomatrixMarine Limited for their assistance, encouragement, and guidance in the use of ANSYS software for this research. Their support and technical advice were invaluable and greatly contributed to the successful completion of this work. The author truly appreciates their commitment to knowledge sharing and professional development in marine and offshore engineering applications

REFERENCES

[1] B. B. Mekha, "New Frontiers in the Design of Steel Catenary Risers for Floating Production Systems," *Journal of Offshore Mechanics and Arctic Engineering*, vol. 123, no. 4, pp. 153–158, Nov. 2001, doi: 10.1115/1.1410101.
[2] C. V. Amaechi, C. Chesterton, H. O. Butler, F. Wang, and J. Ye, "An Overview on Bonded Marine Hoses for Sustainable Fluid Transfer and (Un)Loading Operations via Floating Offshore Structures (FOS)," *J. Mar. Sci. Eng.*, vol. 9, no. 11, p. 1236, Nov. 2021, doi: 10.3390/jmse9111236.
[3] X. Ju, C. V. Amaechi, B. Dong, X. Meng, and J. Li, "Numerical analysis of fishtailing motion, buoy kissing and pullback force in a catenary anchor leg mooring (CALM) moored tanker system," *Ocean Engineering*, vol. 278, p. 114236, Jun. 2023, doi: 10.1016/j.oceaneng.2023.114236.
[4] Q. Yin *et al.*, "Simulation and Optimization of Coupling Dynamic Response of Steel Catenary Riser for a Semi-Submersible Platform Under Harsh Conditions in the South China Sea," *China Ocean Engineering*, vol. 39, no. 5, pp. 917–927, Oct. 2025, doi: 10.1007/s13344-025-0071-0.
[5] R. A. Khodr, R. S. Shiban, B. A. Nawaz, and S. P. Mistry, "Reliability of Very Large Crude Carrier and Single Anchor Leg Mooring Buoy Mooring System During Squall Event," in *Offshore Technology Conference*, OTC, May 2020. doi: 10.4043/30489-MS.
[6] S. Ma, M. H. Kim, and S. Shi, "Second-Order Low-Frequency Wave Forces on a SPM Offloading Tanker in

[7] Shallow Water," *Journal of Offshore Mechanics and Arctic Engineering*, vol. 131, no. 4, Nov. 2009, doi: 10.1115/1.3160519.

[8] C. Y. Ma, U. Alibrandi, and C. G. Koh, "Reliability Analysis of a Steel Catenary Riser With Environmental, Geometry, and Operational Uncertainties," in *Volume 4A: Structures, Safety and Reliability*, American Society of Mechanical Engineers, Jun. 2014. doi: 10.1115/OMAE2014-23057.

[9] K.-S. Park, H.-S. Choi, D.-K. Kim, S.-Y. Yu, and S.-C. Kang, "Structural Analysis of Deepwater Steel Catenary Riser using OrcaFlex," *Journal of Ocean Engineering and Technology*, vol. 29, no. 1, pp. 16–27, Feb. 2015, doi: 10.5574/KSOE.2015.29.1.016

[10] API, *API 2SK : Design and analysis of stationkeeping systems for floating structures*, 3rd ed. American Petroleum Institute, 2005.

[11] M. Dogliani and A. Pittaluga, "Extreme Surge And Mooring Load Of Fps Structures," in *Offshore Technology Conference*, OTC, May 1993. doi: 10.4043/7198-MS.

[12] J. L. Meriam, , L. G Kraige, and J. N. Bolton, *Engineering mechanics: Dynamics*, 8th ed., vol. 2. Hoboken,: John Wiley & Sons, Inc, 2015.

[13] X. Zhang, J. Hu, and B. Hong, "Dynamic Response Computation of Single-Point Mooring of Product Tanker Based on AQWA," *IOP Conf. Ser. Earth Environ. Sci.*, vol. 527, no. 1, p. 012010, Jul. 2020, doi: 10.1088/1755-1315/527/1/012010.

[14] ANSYS, *Aqwa theory manual*. Canonsburg, PA 15317: ANSYS, Inc. Southpointe, 2025.

[15] G. Z. Forristall, K. Ewans, M. Olagnon, and M. Prevosto, "The West Africa Swell Project (WASP)," in *Volume 2B: Structures, Safety and Reliability*, American Society of Mechanical Engineers, Jun. 2013. doi: 10.1115/OMAE2013-11264.

[16] Birbanescu-Biran and R. L. Pulido, *Ship Hydrostatics and Stability*, 2nd ed. Oxford: Butterworth-Heinemann, 2014.

[17] S. J. Banfield, N. F. Casey, and R. Nataraja, "Durability of Polyester Deepwater Mooring Rope," in *Offshore Technology Conference*, OTC, May 2005. doi: 10.4043/17510-MS.

[18] D. Qiao, J. Yan, H. Liang, D. Ning, B. Li, and J. Ou, "Analysis on snap load characteristics of mooring line in slack-taut process," *Ocean Engineering*, vol. 196, p. 106807, Jan. 2020, doi: 10.1016/j.oceaneng.2019.106807.

[19] A. Subbulakshmi and M. Verma, "Dynamic response analysis of a semisubmersible floating offshore wind turbine subjected to mooring line failure under normal and extreme environmental conditions," *Ocean Engineering*, vol. 304, p. 117907, Jul. 2024, doi: 10.1016/j.oceaneng.2024.117907.

[20] S. Hao, X. Zhang, Y. Yu, B. Wang, and X. Bo, "Mooring Failure Analysis of Semisubmersible Floating Offshore Wind Turbines Considering Mooring Redundancy at Each Azimuth Angle," *J. Mar. Sci. Eng.*, vol. 13, no. 2, p. 360, Feb. 2025, doi: 10.3390/jmse13020360.

[21] S. Chandrasekaran and S. A. Uddin, "Postulated failure analyses of a spread-moored semi-submersible," *Innovative Infrastructure Solutions*, vol. 5, no. 2, p. 36, Aug. 2020, doi: 10.1007/s41062-020-0284-2.

[22] K. Xu, K. Larsen, Y. Shao, M. Zhang, Z. Gao, and T. Moan, "Design and comparative analysis of alternative mooring systems for floating wind turbines in shallow water with emphasis on ultimate limit state design," *Ocean Engineering*, vol. 219, p. 108377, Jan. 2021, doi: 10.1016/j.oceaneng.2020.108377.